Tellus (1987), *39A*, 61–71

A model study of pure katabatic flows

By CARMEN J. NAPPO and K. SHANKAR RAO, *Atmospheric Turbulence and Diffusion Laboratory, NOAA, P.O. Box-E, Oak Ridge, Tennessee 37831, USA*

(Manuscript received July 9, 1985; in final form February 12, 1986)

ABSTRACT

A time-dependent 2-dimensional model of pure katabatic flow over a simple finite-length slope is described. This numerical model, based on a turbulent kinetic energy closure, accounts for the effects of radiative cooling and turbulent friction at the surface, and entrainment of air aloft from a quiescent stably stratified ambient atmosphere. The model provides information on the temporal and spatial evolution and structure of katabatic flows.

Numerical solution of the governing equations facilitates explicit determination of the coefficient of entrainment, slope Richardson number, profile-shape factors, and depth, velocity, and buoyancy-deficit scales of the flow. The steady-state results of the model, showing the variations of these parameters as functions of downslope distance, slope angle, and ambient stratification, are presented and discussed. For near-neutral stratification, the calculated entrainment coefficient varies as a function only of the slope Richardson number, in agreement with laboratory data. As ambient stratification increases, it profoundly affects the structure of the flow by reducing its depth, speed and entrainment rate. The results and parameterizations presented here can be used as inputs to hydraulic models of drainage flow and pollutant transport.

1. Introduction

The pure katabatic flow considered in this paper refers to a local gravity current resulting from radiative cooling of the surface of a finite open slope in the absence of an ambient wind. An understanding of the physical processes, structure, and behavior of this simple flow is necessary in order to predict and parameterize its important properties for use in models of drainage flow and pollutant transport and dispersion in complex terrain, such as those described by Yamada (1981) and McNider and Pielke (1984).

Several analytical and numerical model studies of pure katabatic flow have been reported in the literature. Recent summaries and analysis of this work and related references can be found in Manins and Sawford (1979) and Mahrt (1982). One-dimensional katabatic flow models can be broadly classified into two types: (a) models that calculate the vertical structure of flow that is assumed to be invariant in the downslope direction, and (b) models that calculate the downslope variation of integral scales of flow whose vertical structure is assumed to be self-similar.

Prandtl's (1942) one-dimensional model of the stationary slope wind is an example of the first type of models in which the advection terms are neglected. Prandtl's analytical solutions for wind and temperature profiles show good agreement with field observations (Defant, 1949; Lettau, 1966; Hootman and Blumen, 1983) and with predictions from a numerical model with height and stability-dependent eddy diffusivities (Rao and Snodgrass, 1981) based on the local turbulent kinetic energy. These models should yield satisfactory results for katabatic flow over long uniform slopes, away from ridges and valleys, when the advection effects are small (Gutman, 1972). Garrett (1983) and Doran and Horst (1983) modified this type of one-dimensional model to account for downslope variation of flow by approximating the advection terms in the governing equations by their slope-averaged values.

The second type of models are exemplified by the pioneering work of Ellison and Turner (1959), who extended the hydraulic modeling approach of Fleagle (1950) and Ball (1956) to include the interfacial entrainment of ambient fluid into the katabatic flow, and conducted laboratory experiments to determine the entrainment rates. Based on this extended hydraulic approach, Manins and Sawford (1979) and Briggs (1981) developed models that calculate the downslope development of the "average" conditions in pure katabatic flow over an open slope of finite length. The turbulent entrainment in these models is specified a priori through parameterizations based on the laboratory data of Ellison and Turner (1959). However, it has not been established that the relationships between the entrainment coefficient and the layer Richardson number obtained from these laboratory experiments are applicable to atmospheric katabatic flows under all ambient conditions.

More realistic simulations of katabatic flows are afforded by two-dimensional models which numerically solve the governing differential equations. These models are considerably more general than the highly parameterized analytical or one-dimensional numerical models. In this paper, we describe a time-dependent two-dimensional katabatic flow model based on a turbulent kinetic energy closure, which provides information on the spatial variation of the flow as a function of time. The steady-state predictions of this numerical model are utilized to evaluate and examine the variations of the entrainment coefficient, and the flow depth, velocity, and buoyancy-deficit scales as functions of downslope distance, slope angle, and ambient stratification. These results are presented and discussed in relation to the physics of katabatic flows.

2. Numerical model

We consider a pure katabatic flow down a uniform open slope of length L and inclination β to the horizontal, and adopt a slope-aligned coordinate system (s, y, n) with its origin at the crest of the slope, such that the s-axis is oriented along the fall-line vector and the n-axis is normal to the slope. The governing equations of the two-dimensional flow are then given as follows:

$$\frac{\mathrm{D}u}{\mathrm{D}t} = -\frac{g}{\theta_0}\theta' \sin\beta + \frac{\partial}{\partial n}\left(K_m \frac{\partial u}{\partial n}\right) + \frac{g}{\theta_0}\cos\beta \frac{\partial}{\partial s}\left(\int_n^{h_r} \theta' \, \mathrm{d}n\right), \tag{1}$$

$$\frac{\mathrm{D}\theta'}{\mathrm{D}t} = \gamma(u \sin\beta - w\cos\beta) + \frac{\partial}{\partial n}\left(K_\mathrm{h}\frac{\partial \theta'}{\partial n}\right), \tag{2}$$

$$\frac{\partial u}{\partial s} + \frac{\partial w}{\partial n} = 0, \tag{3}$$

where $\mathrm{D}/\mathrm{D}t = \partial/\partial t + u\,\partial/\partial s + w\,\partial/\partial n$, and u and w are the downslope and normal velocity components, respectively; $\theta' = \theta - \theta_0$ is the deviation of the mean potential temperature from an undisturbed reference state temperature profile $\theta_0(z)$, defined such that $\mathrm{d}\theta_0/\mathrm{d}z = \gamma = \text{constant}$; g is gravitational acceleration, and h_r is a reference height where u and θ' are zero. We assume that most of the net radiation flux in the surface energy balance goes into removal of sensible heat from the air next to the ground through turbulent transfer, and that net radiation flux divergence in eq. (2) is negligible since the katabatic layer is thin and transparent to radiation.

The eddy diffusivities for momentum and heat are calculated from

$$K_{\mathrm{m,h}} = l_{\mathrm{m,h}}(0.2e)^{1/2}, \tag{4}$$

and the turbulent mixing lengths are given by

$$l_{\mathrm{m,h}} = kn/\phi_{\mathrm{m,h}}, \tag{5}$$

where k is the von Kármán constant and e is the turbulent kinetic energy (TKE). The nondimensional mean velocity and potential temperature gradients, ϕ_m and ϕ_h, are specified according to the similarity relations given by Businger et al. (1971), with $\zeta' = n/L'$, where L' is the local Monin-Obukhov stability length. It should be noted that, for both stable and unstable conditions, ζ' can be conveniently expressed in terms of the local gradient Richardson number which is calculated directly from the model. The TKE is calculated from the equation,

$$\frac{\mathrm{D}e}{\mathrm{D}t} = \frac{\partial}{\partial n}\left(K_\mathrm{m}\frac{\partial e}{\partial n}\right) + K_\mathrm{m}\left(\frac{\partial u}{\partial n}\right)^2 - \frac{g}{\theta_0}K_\mathrm{h}\left(\frac{\partial \theta'}{\partial n} + \gamma\cos\beta\right) - \frac{b(0.2e)^2}{K_\mathrm{m}}, \tag{6}$$

where b is a constant of order unity. The turbulent closure model outlined in eqs. (4) to (6) follows the work of Delage (1974), Nieuwstadt and Driedonks (1979), and Rao and Snodgrass (1981).

At $n = z_0$, the surface aerodynamic roughness height, the lower boundary conditions are

$$u = w = \frac{\partial e}{\partial n} = 0, \tag{7}$$

$$\theta' = -\Delta_0 \quad \text{or} \quad K_h \frac{\partial \theta'}{\partial n} = -Q_0,$$

where $\Delta_0(t)$ is the magnitude of the surface cooling, and $Q_0(t)$ is the surface heat flux defined such that $\Delta_0(0) = Q_0(0) = 0$. At $n = h_r$, the upper boundary conditions are

$$u = \frac{\partial w}{\partial n} = \theta' = e = 0. \tag{8}$$

At the crest of the slope ($s = 0$), the inflow boundary conditions are

$$u = w = \theta' = e = 0, \tag{9}$$

and at $s = L$, the outflow boundary conditions are specified as

$$\frac{\partial}{\partial s}(u, w, \theta', e) = 0. \tag{10}$$

At $t = t_0 \sim 0.25$ h, the flow is initialized by specifying approximate initial profiles for the variables from Prandtl's (1942) analytical solutions. The correct initial conditions at t_0 are then obtained by integrating the model equations, while holding the lower boundary conditions constant, until equilibrium distributions consistent with our formulations evolve. At $t > t_0$, the simulation is started by uniformly decreasing the surface temperature in time until the specified ground temperature-deficit, Δ_0, is attained; from then on, Q_0 is held constant with respect to time, and the numerical integration is continued until a steady state is established, usually at $t = 3$ or 4 h.

The computational grid, using a uniform spacing along the s-axis and logarithmic spacing along the n-axis, covers a domain of 1500 m × 300 m with 31 × 31 points. A time-splitting technique is used whereby the turbulent diffusion contributions to the predicted variables are computed using a Crank-Nicolson finite difference scheme for the first half of the time step, and the downslope advection contributions are calculated using a Chapeau function technique for the second half. Although unconditionally stable, the semi-implicit diffusion scheme requires time steps as small as about 1 s for realistic solutions. Therefore, this primitive equation model must be considered a research tool, because operational use of its code is rather expensive, and requires a large main-frame computer.

This numerical model has been successfully applied to simulate the mean wind and temperature profiles observed by Doran and Horst (1983) in a drainage flow over a nearly two-dimensional slope on Rattlesnake Mountain near Richland, Washington. A comparison of the model results with field observations can be found in Rao and Nappo (1983), and hence will not be given here.

3. Hydraulic model approach

Our model results are more conveniently presented and clearly discussed in terms of scale parameters of the flow rather than in terms of vertical profiles of flow variables; also, these scale quantities allow direct comparison of our results with those obtained from the one-dimensional models of Ellison and Turner (1959), Manins and Sawford (1979), and Briggs (1981). In anticipation of this, we present here a brief discussion of the so-called hydraulic approach in which the vertical structure is eliminated by integration from the surface to the top of the katabatic layer. The characteristic scales of flow velocity (U), momentum thickness (H), and buoyancy-deficit (g') are defined by the integrals,

$$UH = \int_{z_0}^{h} u \, \mathrm{d}n, \quad U^2 H = \int_{z_0}^{h} u^2 \, \mathrm{d}n,$$
$$UHg' = \int_{z_0}^{h} -\left(\frac{g}{\theta_0}\right) \theta' u \, \mathrm{d}n, \tag{11}$$

where UH, $U^2 H$, and UHg', represent the downslope fluxes of flow volume, momentum, and net buoyancy-deficit respectively, and h is the normal height where u first goes to zero.

Integrating eqs. (1) to (3) with respect to n, the steady state equations of the hydraulic model can be obtained as follows:

$$\frac{\mathrm{d}}{\mathrm{d}s}(U^2 H + 0.5 S_1 g' H^2 \cos\beta)$$
$$= S_2 g' H \sin\beta - C_D U^2, \tag{12}$$

$$\frac{\mathrm{d}}{\mathrm{d}s}(Ug'H) = -N^2 UH(\sin\beta + S_3 E\cos\beta) + \frac{g}{\theta_0} Q_0, \tag{13}$$

$$\frac{\mathrm{d}}{\mathrm{d}s}(UH) = EU. \tag{14}$$

In the above $C_D = -\overline{u'w'}/U^2$ is the surface drag coefficient, $Q_0 = -(\overline{w'\theta'})_0$ is the sensible heat flux at the surface, $N = (g\gamma/\theta_0)^{1/2}$ is the Brunt-Väisälä frequency in the ambient atmosphere, and E is the coefficient of entrainment defined by

$$E = -w(h)/U, \tag{15}$$

where $w(h)$ is the entrainment velocity normal to the slope at the top of the katabatic layer, determined by numerical integration of the continuity equation (3). The profile-shape factors S_1, S_2, and S_3, which account for the vertical distributions of u, θ', and w, respectively are defined by

$$S_1 g' H^2 = 2\int_{z_0}^{h} -\left(\frac{g}{\theta_0}\right)\theta' n\,\mathrm{d}n,$$

$$S_2 g' H = \int_{z_0}^{h} -\left(\frac{g}{\theta_0}\right)\theta'\,\mathrm{d}n, \tag{16}$$

$$S_3\, w(h)\, H = \textstyle\int_{z_0}^{h} w\,\mathrm{d}n.$$

In the hydraulic model approach, eqs. (12)–(14) are solved for H, U, and g' by assuming that E, C_D, Q_0 and the profile-shape factors are known a priori. The entrainment coefficient and profile-shape factors are usually specified from the laboratory data of Ellison and Turner (1959). The surface drag coefficient is specified from related field observations. The surface buoyancy flux, $B = gQ_0/\theta_0$ in eq. (13), is generally assumed to be a known constant (Manins and Sawford, 1979; Briggs, 1981) for simplicity.

4. Results and discussion

The two-dimensional fields of mean velocity, $u(s,n)$, and temperature deficit, $\theta'(s,n)$, calculated by our primitive equation model facilitate the explicit evaluation of characteristic scales H, U, and g' of the flow from eq. (11), entrainment coefficient E from eq. (14), and profile-shape factors S_1, S_2, and S_3 from eq. (16). The emphasis in this paper is on examining the variations of these parameters in a steady katabatic flow as functions of the downslope distance, slope angle, and ambient stratification. The steady-state results of the numerical model calculated for $\Delta_0 = 4$°C and $z_0 = 0.1$ m, are presented and discussed in this section. The other model parameters, namely β and γ, are varied as discussed below.

4.1. Near-neutral stratification

Many of the previous studies of katabatic flows dealt with neutral ambient stratification, $\gamma = 0$, which offers the simplest mathematical analysis. In this study, this case is simulated by using a small value of $\gamma = 0.1$ °C/km, because Prandtl's (1942) analytical solutions (used to initialize the model) become singular for $\gamma = 0$. The steady state vertical profiles of u and θ' are numerically integrated at 50 m intervals downslope from the crest to evaluate the scale parameters of the flow discussed below.

The downslope variations of scale height H and scale velocity U are shown in Figs. 1a, b, respectively, as functions of the slope angle β ranging from 2.5° to 40°. After an initial rapid rise in the near-crest region, the scale height H increases linearly with downslope distance s for all slope angles. All other height scales derived from the velocity profiles, such as n_{max} (where the maximum velocity u_{max} occurs) and h (where the velocity goes to zero) are also found to grow linearly with s. The scale velocity U shown in Fig. 1b increases with s at less than a linear rate. As the slope angle increases, both H and U also increase as shown.

The surface heat flux Q_0 has been held constant with time in the model after the specified ground temperature-deficit, $\Delta_0 = 4$°C, is attained. The steady state downslope variation of Q_0 thus calculated is shown in Fig. 2. After an initial rapid increase in the near-crest region, Q_0 increases nearly linearly with s (varying by less than 20% for $400 \leqslant s \leqslant 1500$ m) for all slope angles as shown. From dimensional analysis, the scale parameters H, U, and g' of the katabatic flow, calculated for $s \geqslant 400$ m for the near-neutral stratification case, can be parameterized as follows:

$$H = C_1(\sin\beta)^{2/3} s, \tag{17}$$

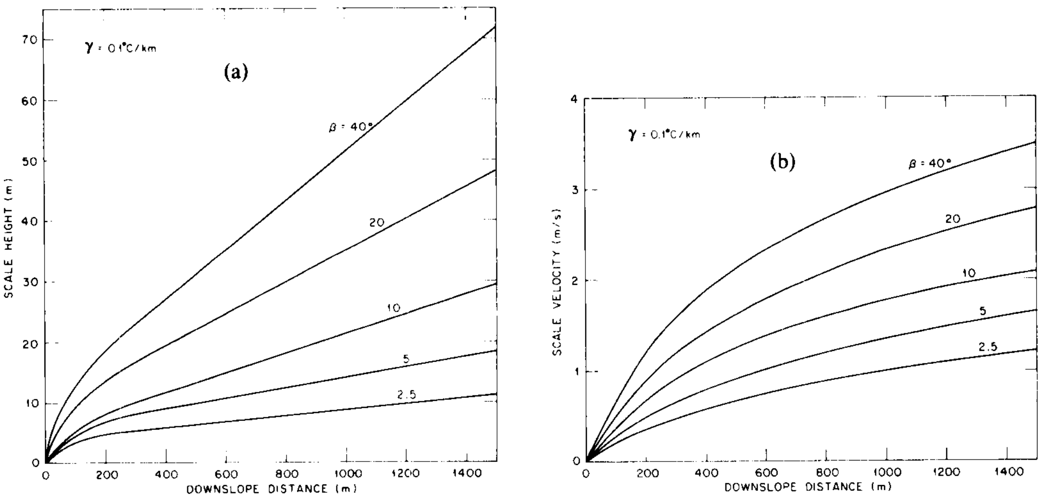

Fig. 1. Variations of scale parameters of steady katabatic flow as functions of downslope distance and slope angle β for near-neutral ambient stratification: (a) height H, and (b) velocity U.

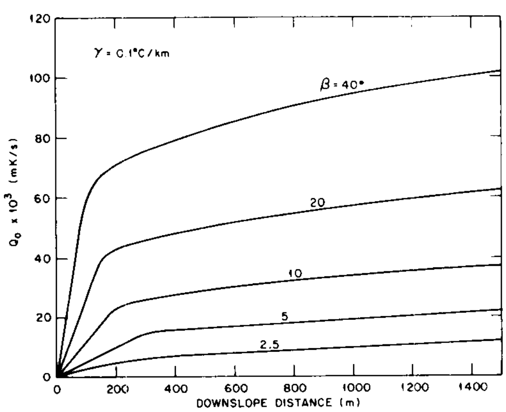

Fig. 2. Calculated variation of turbulent heat flux at surface Q_0 as a function of downslope distance and slope angle β for a surface temperature-deficit $\Delta_0 = 4$°C and roughness length $z_0 = 0.1$ m.

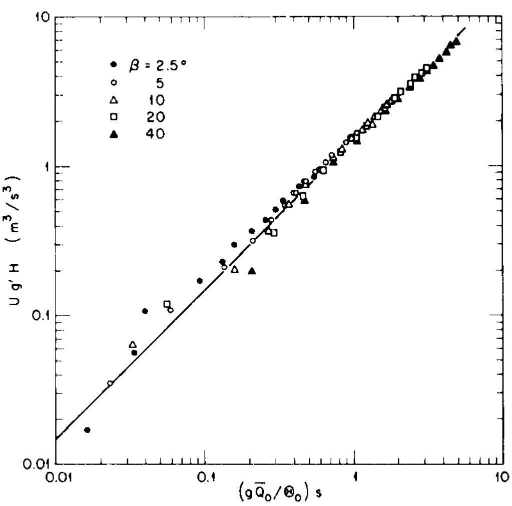

Fig. 3. Variation of the net buoyancy-deficit flux in the steady katabatic flow for near-neutral ambient stratification, see eq. (20).

$$U = C_2 (\sin\beta)^{2/9} \left(\frac{g}{\theta_0} \overline{Q}_0 s\right)^{1/3}, \tag{18}$$

$$g' = C_3 (\sin\beta)^{-8/9} \left(\frac{g}{\theta_0} \overline{Q}_0\right)^{2/3} s^{-1/3}, \tag{19}$$

where C_1, C_2, and C_3 are constants, and $\overline{Q}_0$ is the slope-averaged heat flux. From these expressions, we can write

$$Ug'H = C_4 \left(\frac{g}{\theta_0} \overline{Q}_0\right) s, \tag{20}$$

where C_4 is a constant. Thus, the flux of net buoyancy-deficit at any location downslope is proportional to the downslope distance and the slope-averaged surface heat flux. The plot of $Ug'H$ versus $(g\overline{Q}_0/\theta_0)s$ shown in Fig. 3 supports eq. (20). Similar plots for H, U, and g' separately (not shown) verify that the flow parameters calculated for the near-neutral stratification case

Table 1. *Values of constants in eqs. (17) to (20)*

	Present study	Manins & Sawford (1979)	Briggs (1981)
C_1	0.073	0.075	0.037
C_2	2.5	2.15	2.15
C_3	8.2	6.2	12.6
C_4	1.5	1.0	1.0

follow the scaling laws given in eqs. (17) to (19) fairly well. These equations agree with those derived by Briggs (1981) from a simple analytical model of the katabatic flow with a constant Q_0 and $\gamma = 0$. Manins and Sawford (1979) also gave similar equations for this case in a non-dimensional form; the constants in these equations can be determined utilizing the expressions for E and Ri given later in this section. The values of the constants from various studies are listed in Table 1.

The downslope variation of entrainment coefficient E for various slope angles are shown in Fig. 4. The values of E calculated from both eqs. (14) and (15) are nearly identical, thus providing an independent check on the accuracy of the numerical procedures used in this study. Near the crest of the slope where the flow is assumed to originate, the large values of E result from the small values for the downslope velocity; however, E decreases rapidly with s in this region. Away from the crest ($s > 400$ m), E is approximately constant with downslope distance, especially for $\beta > 10°$, as indicated by previous studies. From eqs. (14), (17), and (18), an analytical expression for the entrainment coefficient in the near-neutral stratification case can be derived as

$$E = 0.10(\sin\beta)^{2/3}, \tag{21}$$

i.e., E approaches a constant value which is independent of s, as shown in Fig. 4.

A measure of the stabilizing effect of the temperature gradient relative to the shear in the katabatic layer is given by the layer or slope Richardson number defined by Ellison and Turner (1959) as

$$\mathrm{Ri} = \frac{g'H}{U^2}\cos\beta, \tag{22}$$

which is the inverse of the internal Froude number of the flow. The downslope variation of Ri,

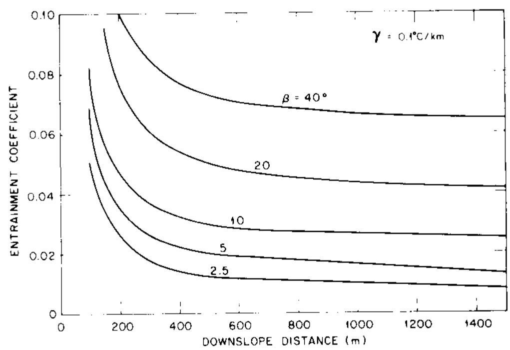

Fig. 4. Downslope variation of entrainment coefficient as function of slope angle β for near-neutral ambient stratification.

calculated from the numerical model results for the near-neutral stratification case, is shown in Fig. 5a for various slope angles. It is clear that Ri rapidly decreases in the near-crest region and, for $s > 400$ m, approaches a constant value which varies inversely with the slope angle. These results are in qualitative agreement with Ellison and Turner's experimental data. Substituting eqs. (17) to (19) in eq. (22), we obtain

$$\mathrm{Ri} = \frac{0.10\cos\beta}{(\sin\beta)^{2/3}}, \tag{23}$$

which closely approximates the constant values of Ri in Fig. 5a for $\beta \geqslant 10°$.

An important conclusion of Ellison and Turner's (1959) laboratory experiments is that the entrainment coefficient is a function only of the slope Richardson number. A comparison of our numerical model results of E versus Ri with Ellison and Turner's laboratory data is shown in Fig. 5b, where the curve labeled "calculated" uses the slope-averaged values of E and Ri for $600 \leqslant s \leqslant 1500$ m, and the curve labeled "parameterized" uses the E and Ri values given by eqs. (21) and (23), respectively. Our calculated E values are slightly larger than the corresponding results of Ellison and Turner for $UHg' =$ constant, but are well within the range of uncertainty of their measurements. Thus we conclude that, for near-neutral ambient conditions, E is solely a function of Ri, and can be estimated from the simple relation

$$E = \frac{0.01\cos\beta}{\mathrm{Ri}} \tag{24}$$

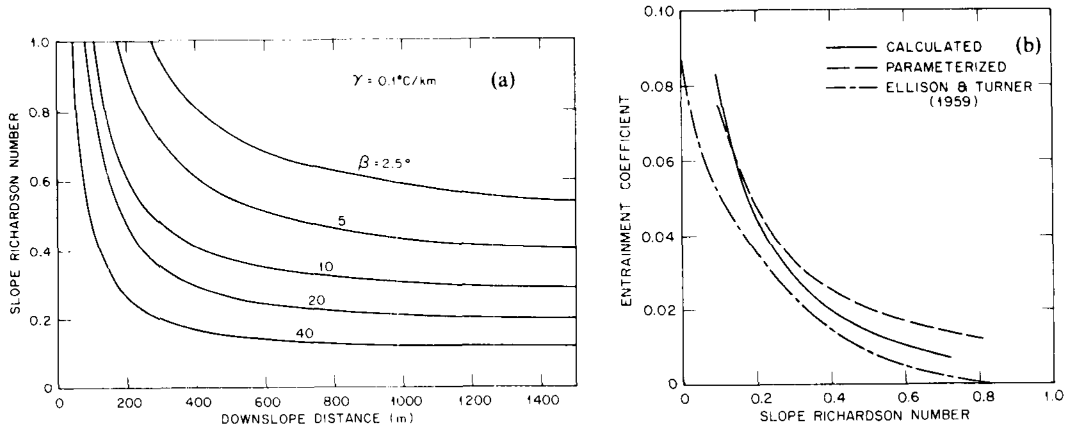

Fig. 5. (a) Variation of slope Richardson number in steady katabatic flow as a function of downslope distance and slope angle β, and (b) variation of entrainment coefficient with slope Richardson number for near-neutral ambient stratification.

derived from eqs. (21) and (23). This expression agrees well with our calculated results, especially for $\beta > 10°$. It should be noted that eq. (24) is not applicable to low slopes corresponding to high values of Ri approaching the "critical" value at which the entrainment vanishes.

4.2. *Effects of ambient stratification*

The effects of increased ambient stratification on steady katabatic flow behavior are investigated over a wide range of γ values between near-adiabatic and isothermal conditions. Fig. 6 compares the vertical profiles of velocity, temperature-deficit, and TKE calculated at $s = 1300$ m for $\beta = 20°$ with two contrasting stratifications, $\gamma = 0.1$ and $\gamma = 10$°C/km. The scale parameters U and H are also shown for comparison. It is apparent that the flow is considerably shallower and weaker for the strong stratification case; the maximum velocity u_{max} is only about half its value for the neutral case. The larger stratification results in the downslope advection and entrainment of warmer ambient air, which acts to decrease the temperature-deficit in the layer; this in turn reduces the katabatic acceleration and the flow speed.

More importantly, for $\gamma = 10$°C/km, the profiles of u and θ' become invariant with increasing downslope distance, and the steady flow becomes essentially one-dimensional, as the downslope advection and entrainment vanish. In this limit,

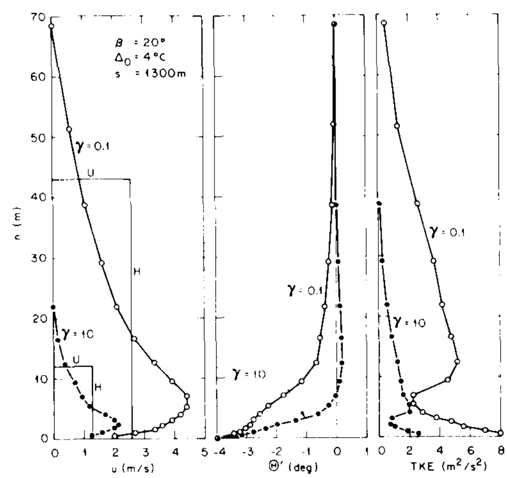

Fig. 6. Comparison of vertical profiles of velocity, temperature-deficit, and turbulent kinetic energy in steady katabatic flow calculated for near-neutral ($\gamma = 0.1$°C/km) and isothermal ($\gamma = 10$°C/km) ambient stratifications.

the governing equations (1) to (3) reduce to

$$\frac{d}{dn}\left(K_m \frac{du}{dn}\right) = \frac{g}{\theta_0}\theta' \sin\beta,$$
$$\frac{d}{dn}\left(K_h \frac{d\theta'}{dn}\right) = u\gamma \sin\beta. \tag{25}$$

Thus, the katabatic force is exactly balanced by the turbulent friction, and the turbulent heat flux divergence is balanced by the downslope-warming due to the ambient stratification. These are also the assumptions made by Prandtl (1942) in formulating his analytical model for the stationary slope wind. Our results show that, as this Prandtl flow condition is approached, both the surface heat flux and the surface stress approach constant values along the slope.

The downslope variations of H, U, and E for various slope angles and $\gamma = 10°C/km$ are plotted in Figs. 7a, b, and c, respectively. For $\beta < 10°$, these curves are similar in shape to the near-neutral case curves, i.e., $H \sim s$, $U \sim s^{1/3}$, and $E \to$ constant. However, the magnitudes of these parameters are considerably reduced from their neutral case values for all slope angles. For $\beta > 10°$, H approaches a constant value which varies as an inverse function of β, as shown in Fig. 7a. The entrainment rate decreases continuously with increasing s, and E vanishes when the Prandtl flow condition is attained at a downslope distance which decreases with increasing β. From Fig. 7b, it can be seen that the scale velocities approach a constant value which is not very sensitive to the slope angle. The scale buoyancy-deficits (not shown) also approach a constant value which is independent of β. These results are in agreement with a sensitivity analysis of Prandtl's analytical solutions by Rao and Snodgrass (1981).

Fig. 8 gives the downslope variations of H and U and entrainment coefficient E, calculated with a constant slope angle ($\beta = 20°$), for several values of ambient stratification ranging from near-adiabatic to isothermal conditions. This family of well-behaved curves shows that, as γ increases, H, U, and E decrease uniformly from their near-neutral values until the Prandtl flow condition, characterized by constant values for H and U, and $E \to 0$, is established for $\gamma \geqslant 10°C/km$.

Plots of the slope Richardson number with downslope distance for different values of γ (not

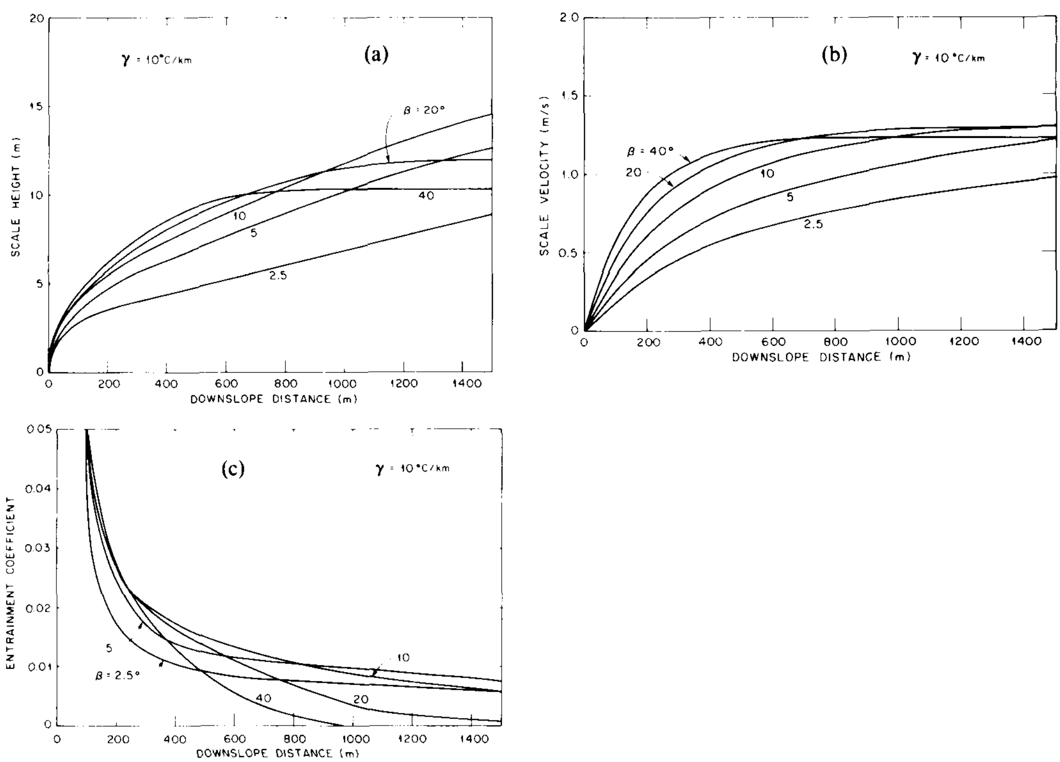

Fig. 7. Variations of the scale parameters in steady katabatic flow as functions of downslope distance and slope angle for strong ambient stratification case: (a) height H, (b) velocity U, and (c) entrainment coefficient E.

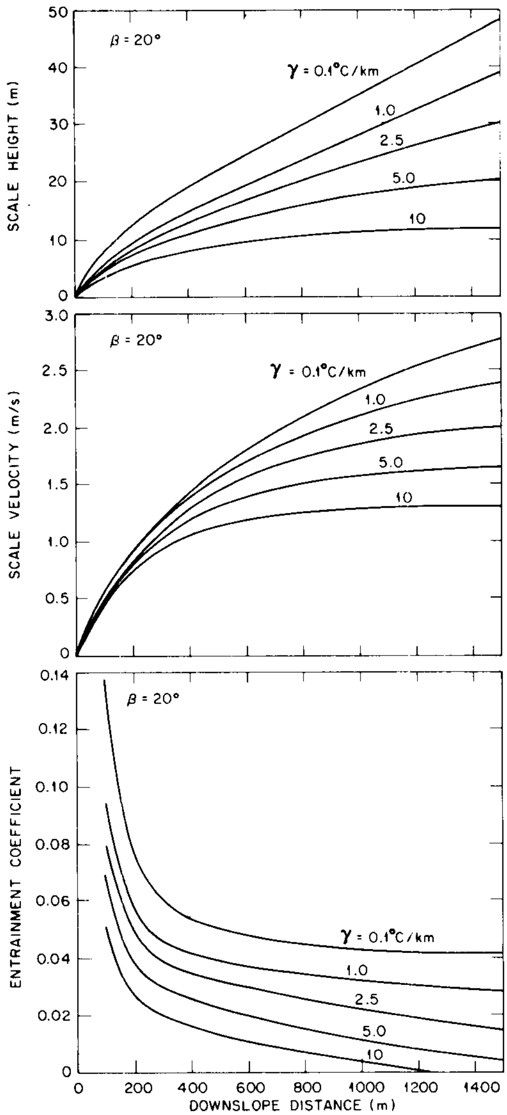

Fig. 8. Variations of scale height, scale velocity, and entrainment coefficient as functions of downslope distance and ambient stratification parameter γ for a constant slope angle $\beta = 20°$.

shown) are essentially the same as those given in Fig. 5a for the near-neutral stratification case. For a given value of β, an increase in γ leads to a decrease in g', U, and H, as shown in Fig. 8, such that $g'H/U^2$ remains constant. Thus we conclude that in the pure katabatic flow, Ri is primarily a function only of the slope angle and is closely approximated by eq. (23).

The entrainment formulations of Manins and Sawford (1979) and Briggs (1981), which assume that E is a sole function of Ri, are based upon the laboratory data of Ellison and Turner (1959). The latter, in their experiments, studied the entrainment of an ambient fluid of uniform density (fresh water) into a jet of salt water injected at the bottom of an inclined tank, thus maintaining a constant flux of buoyancy-deficit along the slope. In the atmospheric case, however, the buoyancy-deficit is created along the slope as the flow loses heat to the radiatively-cooling ground surface. Thus, the net buoyancy-deficit flux increases with downslope distance. Furthermore, in the presence of a stable atmospheric stratification, the downslope advection and entrainment of warmer ambient air destroys the temperature-deficit in the layer until eventually a balance is established between the turbulent heat transfer and the downslope-warming due to ambient stratification. The model results presented in Figs. 7 and 8 demonstrate that E is strongly dependent on ambient stratification; for $\gamma = 10$°C/km and $\beta > 10°$, the entrainment vanishes beyond some distance downslope, and the flow becomes essentially one-dimensional. We speculate that, for sufficiently long slopes, this Prandtl flow regime may be established at even smaller values of β and γ. This condition may not be reached over slopes of finite length if the ambient stratification is not strong enough or if the slope is not sufficiently steep. In such cases, however, we still expect the entrainment coefficient to decrease with downslope distance as shown in Fig. 8. Thus, we conclude that in the general case of an arbitrary ambient stratification, E is a function of Ri, γ, and s.

4.3. Profile-shape factors and flow-scale relations

The profile-shape factors S_1, S_2, and S_3 have not so far been evaluated with any certainty. Ellison and Turner (1959) give values of S_1 between 0.2 and 0.3, and S_2 between 0.6 and 0.9 from laboratory data on inclined plumes. Manins and Sawford (1979) use the data from a field experiment to estimate $S_1 \simeq 0.5$ and $S_2 \simeq 0.9$ for a slope angle of 5°. Little is known about S_3; consequently its value is usually set to unity. The determination of these shape-factors requires detailed temperature and velocity profile data

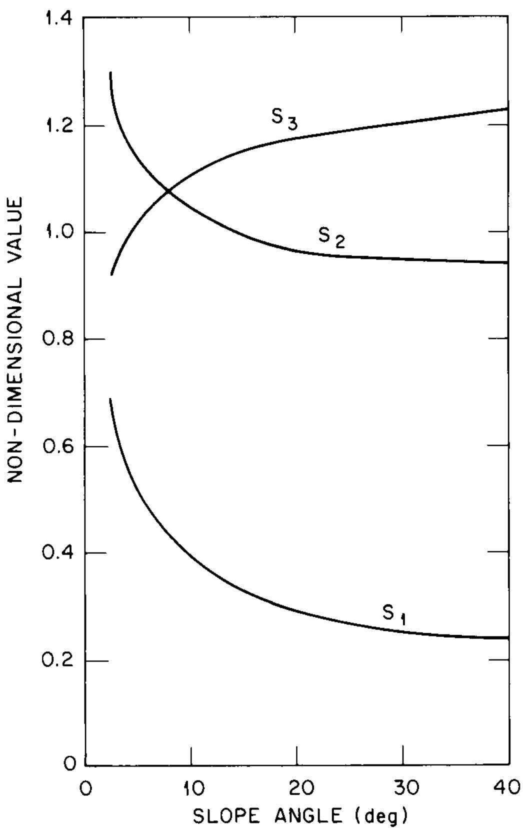

Fig. 9. Calculated variations of profile-shape factors with slope angle.

which are not available. However, our numerical model results permit explicit calculations of these factors from eqs. (11) and (16). Fig. 9 shows the variations of S_1, S_2, and S_3 as functions of the slope angle. The plotted values represent the averages over γ and s, since the calculated shape-factors do not vary significantly with these quantities. It can be seen that, as the slope angle increases, S_1 and S_2 decrease and S_3 increases. For $\beta > 10°$, our results are in agreement with Ellison and Turner's (1959) experimental values. We also note that S_3 is of order unity for moderate slope angles. These results suggest that, in the hydraulic models, one should consider the variation of profile-shape factors with slope angle, especially for $\beta < 10°$.

For practical applications, it may be necessary to estimate the thickness of the katabatic layer (h), the maximum velocity (u_{max}), and the height where it occurs (n_{max}), from a knowledge of the scale parameters U and H. For this purpose, we examined the variations of the ratios U/u_{max}, H/h, and n_{max}/h calculated from our model results. These ratios show little variability with γ and s, and do not vary significantly for $\beta > 10°$. The "average" values of these ratios are given by $U/u_{max} = 0.64$, $H/h = 0.53$, and $n_{max}/H = 0.14$. Thus, for example, given the observed values of the velocity maximum and its height above ground, one may estimate U, H, and h from these relations.

5. Conclusions

The steady state structure of an idealized pure katabatic flow over a finite slope has been investigated using a two-dimensional numerical model based on turbulent kinetic energy closure. It is difficult to observe such gravity driven currents in the field because of the disturbing effects of ambient winds and three-dimensional terrain featues. This high-resolution model, which provides information on the vertical structure as well as the downslope development of the flow as a function of time, is therefore particularly useful for parameterization and sensitivity studies. The model (including the effects of ambient winds) has been previously tested against field data (Rao and Nappo, 1983) and shown to reproduce the observed profiles of wind speed and temperature in the drainage flow over a simple slope.

In this study, the characteristic scales for the katabatic flow depth, velocity, and buoyancy-deficit are calculated, and their variations are examined as functions of downslope distance, slope angle, and ambient stratification. For the near-neutral stratification case, these parameters are shown to vary in accordance with the simple scaling expressions derived from hydraulic models which consider only the vertically averaged flow in the katabatic layer. The numerical model also permits direct evaluation of the entrainment coefficient and profile-shape factors which are needed as input data to the hydraulic models.

The effect of ambient thermal stratification on the katabatic flow is of special interest in this study, because this effect cannot be easily simulated in the laboratory. We have shown that the stratification $\gamma > 0$ profoundly affects the structure of the flow. For sufficiently long or steep slopes, the presence of a moderate to strong ambient stratification results ultimately in a one-dimensional flow regime in which the katabatic flow depth, speed, and buoyancy-deficit become invariant with downslope distance, in accord with Prandtl's (1942) analysis.

Away from the crest region, the layer or slope Richardson number of the flow is found to become a unique constant which depends primarily on the slope angle; this "closed" behavior, which is insensitive to the ambient stratification and the downslope distance, results from the fact that the wind speed and temperature-deficit are uniquely and locally related in a pure katabatic flow. For the near-neutral stratification case, the calculated entrainment coefficient E is shown to vary as an inverse function of only the slope Richardson number, in agreement with Ellison and Turner's (1959) laboratory data. However, in the general case of an arbitrary ambient stratification $\gamma > 0$, our model results show that E is function of Ri, γ, and s.

The results and parameterizations presented here can be used in hydraulic drainage flow and pollutant transport modeling, and for instrument-siting in field experiments.

6. Acknowledgements

This work was performed under an interagency agreement between the National Oceanic and Atmospheric Administration (NOAA) and the US Department of Energy (DOE) as part of DOE's ASCOT program. The authors thank R. P. Hosker, B. B. Hicks, J. M. Godowitch, T. W. Horst, and P. C. Manins for helpful suggestions to improve the manuscript.

REFERENCES

Ball, F. K. 1956. The theory of strong katabatic winds. *Aust. J. Phys. 9*, 373–386.

Briggs, G. A. 1981. Canopy effects on predicted drainage flow characteristics and comparisons with observations. *Proc. 5th Symp. on Turb. and Diff.*, Atlanta. Amer. Meteorol. Soc., Boston, MA, 113–115.

Businger, J. A., Wyngaard, J. C., Izumi, Y. and Bradley, E. F. 1971. Flux-profile relations in the atmospheric surface layer. *J. Atmos. Sci. 28*, 181–189.

Defant, F. 1949. Zur theorie der hangwinde, nebst bemerkungen zur theorie der berg-und talwinde. *Arch. Meteorol. Geophys. Biokl., A1*, Springer-Verlag, 421–450.

Delage, Y. 1974. A numerical study of nocturnal atmospheric boundary layer. *Q. J. R. Meteorol. Soc. 100*, 351–364.

Doran, J. C. and Horst, T. W. 1983. Observations and models of simple nocturnal slope flows. *J. Atmos. Sci. 40*, 708–717.

Ellison, T. H. and Turner, J. S. 1959. Turbulent entrainment in stratified flows. *J. Fluid Mech. 6*, 423–448.

Fleagle, R. G. 1950. A theory of air drainage. *J. Meteorol. 7*, 227–232.

Garrett, A. J. 1983. Drainage flow prediction with a one-dimensional model including canopy, soil, and radiation parameterization. *J. Clim. Appl. Meteorol. 22*, 79–91.

Gutman, L. N. 1972. *Introduction to the nonlinear theory of mesoscale meteorological processes. TT 71-50132*, NTIS, Springfield, VA, 224 pp.

Hootman, B. W. and Blumen, W. 1983. Analysis of nighttime drainage winds in Boulder, Colorada during 1980. *Mon. Wea. Rev. 111*, 1052–1061.

Lettau, H. H. 1966. A case study of katabatic flow on the south polar plateau. *Studies in antarctic meteorology*, M. J. Rubin, ed. *Antarc. Res. Ser. 9*, Amer. Geophys. Union, 1–11.

Mahrt, L. 1982. Momentum balance of gravity flows. *J. Atmos. Sci. 39*, 2701–2711.

Manins, P. C. and Sawford, B. L. 1979. A model for katabatic winds. *J. Atmos. Sci. 36*, 619–630.

McNider, R. T. and Pielke, R. A. 1984. Numerical simulation of slope and mountain flows. *J. Clim. Appl. Meteorol. 23*, 1441–1453.

Nieuwstadt, F. T. M. and Driedonks, A. G. M. 1979. The nocturnal boundary layer: A case study compared with model calculations. *J. Appl. Meteorol. 18*, 1397–1405.

Prandtl, L. 1942. Führer durch die Strömungslehre. Vieweg & Sohn, Brunschweig, 373–375. Available in English as *Essentials of fluid dynamics*. Hafner Publishing Co., New York, 1952.

Rao, K. S. and Snodgrass, H. F. 1981. A nonstationary nocturnal drainage flow model. *Bound.-Layer Meteorol. 20*, 309–320.

Rao, K. S. and Nappo, C. J. 1983. Comparison of observations and model predictions of nocturnal drainage flow over a simple slope. *Proc. 6th Symp. on Turb. and Diff.* Boston, Amer. Meteorol. Soc., Boston, MA, 184–187.

Yamada, T. 1981. A numerical simulation of nocturnal drainage flow. *J. Meteorol. Soc. Japan 59*, 108–122.